

CLUSTER REDSHIFTS IN FIVE SUSPECTED SUPERCLUSTERS

ROBIN CIARDULLO

University of California, Los Angeles; and Space Telescope Science Institute

HOLLAND FORD

Space Telescope Science Institute

AND

RICHARD HARMS

Applied Research Corporation, Landover, Maryland

Received 1984 July 18; accepted 1984 December 18

ABSTRACT

Redshift surveys for rich superclusters were carried out in five regions of the sky containing surface-density enhancements of Abell clusters. While several superclusters are identified, projection effects dominate each field, and no system contains more than five rich clusters. Two systems are found to be especially interesting. The first, field 0136–10, is shown to contain a superposition of at least four distinct superclusters, with the richest system possessing a small velocity dispersion. The second system, 2206–22, though a region of exceedingly high Abell cluster surface density, appears to be a remarkable superposition of 23 rich clusters almost uniformly distributed in redshift space between $0.08 < z < 0.24$. The new redshifts significantly increase the three-dimensional information available for the distance class 5 and 6 Abell clusters and allow us to estimate the spatial correlation function around rich superclusters.

Subject headings: galaxies: clustering — galaxies: redshifts

I. INTRODUCTION

Superclusters provide a tool for studying both the past and future of the universe. Since superclusters are unrelaxed, the distribution of matter within them today reflects the initial conditions in the primordial density perturbations. In addition, the motions of the clusters are affected by the overall supercluster potential. Estimates of large-scale matter density are therefore possible from detailed modeling of the observed Hubble expansion. In principle, then, superclusters allow us to probe both the physics of the early universe and the cosmological density parameter Ω_0 .

Although extremely important, data on superclusters are difficult to obtain. Only the nearest superclusters can be studied using whole-sky, magnitude-limited, redshift surveys. For fainter, more distant systems, specific regions of the sky must be singled out for redshift measurements. In order to choose these regions effectively, the areas likely to contain superclusters must first be identified.

Studies of the correlation function for galaxies and clusters (Bahcall and Soneira 1983) suggest that rich clusters are good tracers of large-scale structure. Consequently, the Abell cluster catalog (Abell 1958) provides a useful tool for the study of superclusters. Rood (1976) and Thuan (1980) used samples of nearby Abell clusters with known redshifts to identify probable superclusters out to $z \approx 0.08$ and initiated the first studies of superclusters in three-dimensional space. Unfortunately, most of these systems include only two or three Abell clusters; the very rich associations which may contain five or more Abell clusters are rare. To identify such rich systems, an even larger volume of the universe must be investigated.

The surface density enhancement of Abell clusters provides an effective way to isolate potentially rich systems. Several authors, notably Abell (1961) and Murray *et al.* (1977, hereafter MFJG) have used the projected distributions of Abell clusters on the sky to identify large sets of possible superclusters.

Without some corroborating redshift information, however, the usefulness of these catalogs is limited. The richest superclusters, though present in the catalog, are hidden among systems formed by chance superpositions.

Here, we report the results of a search for rich superclusters through cluster redshift surveys in five regions of the sky containing surface-density enhancements of Abell clusters. In § II we describe our observations and galaxy-selection criteria. In § III we list the cluster redshifts, discuss the completeness of our sample, and state the implications for superclusters in each of the surveyed regions. We conclude by using these data and data from other supercluster surveys to compute the spatial correlation function for Abell clusters in rich superclusters.

II. OBSERVATIONS

Redshifts of galaxies in 62 Abell clusters, most lying in five suspected supercluster fields, were measured over a four-year period. Most of the observations were performed using the image tube scanner (ITS; Miller, Robinson, and Wampler 1976; Miller, Robinson, and Schmidt 1980) on the 3 m telescope at Lick Observatory. The “red” image-tube chain was used in combination with a $600 \text{ lines mm}^{-1}$ grating blazed at 5000 Å in first order to yield spectra with 11 Å resolution. For the southernmost field, the observations were obtained with the SIT vidicon detector at the Ritchey-Chrétien focus of the CTIO 4 m telescope. A $632 \text{ lines mm}^{-1}$ grating blazed at 4200 Å in first order was used, which yielded spectra with 4 Å resolution. The spectra from both telescopes were centered at 5200 Å and covered 2500 Å.

Because the SIT vidicon is a two-dimensional detector, one-dimensional spectral data from this instrument were first extracted using the Tololo-Vienna Reduction System. These data along with all the ITS data were reduced to flux versus log wavelength using the FORTRAN Scanner Data Reduction System (FSDRS; Grandi 1982). Galaxy redshifts were then

TABLE 1
OBSERVING LOG AND HELIOCENTRIC REDSHIFTS

Galaxy (1)	Date (2)	Observatory (3)	α (1950) (4)	δ (1950) (5)	z (6)	Quality (7)
A186-1	1980 Oct 7	Lick	1 ^h 20 ^m 43 ^s .1	-10°40'49"	0.1538	B
A186-2	1980 Oct 7	Lick	1 20 50.1	-10 41 06	0.0992	C+
A188-1	1980 Oct 7	Lick	1 20 12.5	-13 00 20	0.1233	B
A188-2	1980 Nov 10	Lick	1 20 20.2	-13 02 36	0.1227	A-
A190-1	1980 Oct 6	Lick	1 21 13.8	-10 06 50	0.1273	B+
A190-2	1980 Oct 6	Lick	1 21 16.2	-10 04 19	0.1026	B
A190-3	1980 Nov 10	Lick	1 21 07.0	-10 07 23	0.1024	B+
A190-4	1980 Nov 10	Lick	1 21 14.7	-10 05 07	0.0995	B-
A204-1	1980 Oct 8	Lick	1 26 05.7	-7 01 30	0.1557	A-
A204-2	1980 Oct 8	Lick	1 25 45.9	-7 03 39	0.1870	B-
A216-1	1980 Oct 7	Lick	1 34 21.8	-6 42 07	0.1158	A
A217-2	1980 Oct 6	Lick	1 33 52.5	-8 18 12	0.1121	B
A217-3	1980 Oct 6	Lick	1 34 23.0	-8 21 40	0.1131	A-
A224-1	1980 Oct 8	Lick	1 35 48.3	-7 10 35	0.1610	B+
A224-2	1980 Oct 8	Lick	1 35 46.6	-7 11 00	0.1623	B
A226-1	1978 Nov 28	Lick	1 36 21.6	-10 33 45	0.1275	B+
A226-2	1978 Nov 28	Lick	1 36 29.6	-10 29 29	0.1289	A
A226-3	1980 Oct 6	Lick	1 36 33.5	-10 29 54	0.1144	C
A228-1	1978 Nov 29	Lick	1 36 43.0	-10 22 35	0.1296	B+
A228-3	1978 Nov 29	Lick	1 36 39.5	-10 20 11	0.1306	B
A228-4	1979 Oct 22	Lick	1 36 41.8	-10 20 42	0.1245	B
A232-1	1978 Nov 28	Lick	1 37 26.2	-10 35 54	0.1318	A-
A232-2	1978 Nov 28	Lick	1 37 40.6	-10 36 20	0.1889	B-
A232-3	1979 Oct 24	Lick	1 37 43.4	-10 42 40	0.1858	A-
A232-5	1979 Oct 24	Lick	1 37 25.6	-10 36 17	0.1340	B
A236-1	1979 Oct 22	Lick	1 38 04.9	-12 06 50	0.1892	B+
A236-2	1979 Oct 22	Lick	1 38 03.4	-12 07 53	0.1856	B-
A243-1	1978 Nov 29	Lick	1 39 59.0	-10 31 37	0.1110	B
A243-2	1978 Nov 29	Lick	1 39 59.1	-10 31 03	0.1094	B+
A243-3	1978 Nov 29	Lick	1 39 56.5	-10 29 07	0.1140	B
A243-4	1978 Nov 29	Lick	1 39 57.0	-10 31 17	0.1122	A-
A259-1	1980 Oct 6	Lick	1 47 45.6	-12 14 05	0.1307	A-
A259-2	1980 Oct 6	Lick	1 47 50.4	-12 13 56	0.1236	B
A259-3	1980 Oct 6	Lick	1 47 43.8	-12 14 29	0.1276	B
A506-1	1979 Jan 29	Lick	4 40 50.4	-9 46 43	0.1562	B
A506-2	1979 Jan 29	Lick	4 40 35.2	-9 48 57	0.1558	B-
A506-3	1979 Oct 24	Lick	4 40 59.4	-9 46 08	0.1564	B
A513-1	1978 Nov 29	Lick	4 46 02.4	-9 45 58	0.1491	B-
A513-3	1979 Oct 22	Lick	4 46 08.8	-9 45 32	0.1105	A-
A516-2	1979 Jan 29	Lick	4 47 16.5	-8 51 55	0.1396	C
A516-3	1979 Jan 29	Lick	4 47 42.7	-8 50 02	0.1055	C-
A516-4	1979 Nov 16	Lick	4 47 16.4	-8 50 47	0.1418	B-
A517-1	1979 Oct 24	Lick	4 48 12.6	-9 18 32	0.2244	C+
A518-1	1980 Oct 27	Lick	4 48 56.1	-10 49 50	0.1817	B
A518-2	1980 Oct 7	Lick	4 48 55.1	-10 49 45	0.1811	B-
A528-1	1978 Nov 27	Lick	4 56 44.5	-9 06 04	0.2896	C
A528-3	1978 Nov 28	Lick	4 56 57.7	-9 05 46	0.0728	C+
A719-2	1978 Nov 10	Lick	8 59 49.1	+78 13 19	0.2458	B+
A738-1	1980 Nov 12	Lick	9 06 24.1	+78 15 27	0.2143	B+
A738-2	1980 Nov 12	Lick	9 06 19.3	+78 15 22	0.2599	B
A768-1	1980 Nov 12	Lick	9 18 44.8	+79 34 44	0.0765	B-
A777-1	1980 Nov 10	Lick	9 23 25.7	+78 30 09	0.2183	B+
A1283-1	1980 Apr 15	Lick	11 28 43.0	+61 03 39	0.1434	B
A1322-1	1979 Jan 29	Lick	11 33 32.5	+63 31 02	0.1137	B-
A1322-2	1979 Jan 29	Lick	11 33 15.4	+63 31 29	0.1075	A
A1322-3	1979 Jan 29	Lick	11 33 23.7	+63 31 01	0.1101	B
A1343-1	1979 Jan 29	Lick	11 38 08.6	+60 54 53	0.1336	B+
A1343-2	1979 Jan 29	Lick	11 38 25.9	+60 58 19	0.1300	C+
A1359-1	1980 Apr 16	Lick	11 41 14.5	+61 57 45	0.1783	A-
A1859-1	1981 Apr 8	Lick	14 01 13.1	+60 07 11	0.0988	B+
A1872-1	1981 Apr 9	Lick	14 07 34.8	+62 15 38	0.1508	B
A1877-1	1981 Apr 8	Lick	14 09 15.0	+60 05 55	0.1241	B+
A1884-1	1981 Apr 8	Lick	14 07 09.1	+61 23 07	0.1220	A
A1918-1	1981 Apr 6	Lick	14 24 06.9	+63 25 20	0.1380	A-
A1918-2	1981 Apr 6	Lick	14 24 07.3	+63 25 22	0.1392	B+
A1920-1	1981 Apr 7	Lick	14 25 49.4	+55 58 25	0.1310	B+
A1936-1	1981 Apr 7	Lick	14 32 50.4	+55 01 55	0.1386	A-
A1937-1	1981 Apr 7	Lick	14 32 44.8	+58 28 23	0.1382	A
A1940-1	1981 Apr 7	Lick	14 33 54.8	+55 20 55	0.1397	A
A1962-1	1981 Apr 7	Lick	14 41 21.6	+55 20 19	0.1060	B

SUSPECTED SUPERCLUSTERS

71

TABLE 1—Continued

Galaxy (1)	Date (2)	Observatory (3)	α (1950) (4)	δ (1950) (5)	z (6)	Quality (7)
A1975-1	1981 Apr 9	Lick	14 44 33.6	+69 24 27	0.0911	B-
A2000-1	1981 Apr 7	Lick	14 53 17.7	+54 34 37	0.1012	B
A2011-1	1981 Apr 9	Lick	14 58 05.2	+49 59 08	0.1697	B
A2509-1	1981 Sep 1	CTIO	22 55 13.9	-22 01 17	0.2306	B
A2518-1	1981 Oct 2	Lick	22 58 06.6	-24 26 30	0.1351	B
A2521-1	1981 Sep 1	CTIO	22 59 42.6	-22 17 40	0.1391	B+
A2528-1	1981 Sep 1	CTIO	23 02 55.9	-21 39 13	0.0955	A
A2531-1	1981 Sep 1	CTIO	23 04 16.1	-21 56 00	0.1741	A
A2534-1	1981 Sep 1	CTIO	23 05 01.3	-22 58 55	0.1997	B
A2534-2	1981 Sep 1	CTIO	23 05 02.3	-23 00 05	0.1698	A-
A2536-1	1981 Aug 29	CTIO	23 05 06.6	-22 43 46	0.1971	A-
A2538-1	1981 Aug 29	CTIO	23 05 56.3	-20 09 50	0.0817	B-
A2539-1	1981 Sep 1	CTIO	23 06 14.3	-21 45 09	0.1735	A-
A2540-1	1981 Aug 28	CTIO	23 06 45.2	-22 26 33	0.1297	B-
A2541-1	1981 Sep 1	CTIO	23 07 19.9	-23 12 28	0.1018	A ^a
A2542-1	1981 Sep 1	CTIO	23 07 18.2	-24 42 30	0.1603	B+
A2546-1	1981 Aug 29	CTIO	23 07 59.8	-22 55 22	0.1119	B
A2547-1	1981 Aug 28	CTIO	23 08 17.2	-21 24 16	0.1492	B
A2548-1	1981 Aug 29	CTIO	23 08 47.0	-20 40 18	0.1101	B-
A2550-1	1981 Aug 28	CTIO	23 08 56.3	-22 01 04	0.1217	A-
A2554-1	1981 Aug 28	CTIO	23 09 40.5	-21 46 28	0.1094	B+
A2555-1	1981 Aug 28	CTIO	23 10 09.7	-22 26 37	0.1385	A
A2556-1	1981 Aug 28	CTIO	23 10 22.0	-21 54 23	0.0879	A
A2565-1	1981 Aug 28	CTIO	23 13 17.9	-21 24 36	0.1271	A
A2566-1	1981 Aug 28	CTIO	23 13 25.9	-20 44 22	0.0821	A
A2568-1	1981 Aug 28	CTIO	23 14 32.6	-22 30 47	0.1398	A-
0137-112-1	1980 Oct 7	Lick	1 37 31.2	-11 12 01	0.1781	B
0132-106-1	1980 Oct 7	Lick	1 30 57.0	-10 41 41	0.1130	B
0132-106-2	1980 Oct 7	Lick	1 32 08.1	-10 35 08	0.1116	B
0133-105-1	1981 Oct 2	Lick	1 33 20.0	-10 27 49	0.1686	B
0146-121-1	1980 Nov 12	Lick	1 45 48.2	-12 04 42	0.1252	C
0128-111-1	1980 Oct 8	Lick	1 27 51.7	-11 07 33	0.1273	B+
0123-110-1	1980 Oct 8	Lick	1 22 47.8	-10 57 27	0.1071	B-
0123-110-2	1980 Oct 10	Lick	1 22 43.6	-10 57 34	0.1081	B
0123-128-1	1980 Nov 12	Lick	1 22 58.7	-12 50 07	0.1824	C+
0127-108-1	1980 Nov 12	Lick	1 26 41.4	-10 46 57	0.1209	A-
0125-110-1	1980 Nov 12	Lick	1 24 31.2	-11 00 57	0.1265	A-
0137-064-1	1980 Nov 12	Lick	1 37 25.3	-6 24 46	0.1385	B+
0140-069-1	1980 Nov 10	Lick	1 39 38.2	-6 56 49	0.1242	B+

^a Redshift of galaxy Abell 2541 — 1 was measured using its very strong [O II] $\lambda 3727$ emission.

measured using techniques described in an earlier paper (Ciardullo *et al.* 1983, hereafter Paper I).

In all cases we attempted to observe the first-ranked galaxy in the cluster. This was not always the brightest galaxy projected in the cluster field. In order to reduce the possibility of observing foreground or background objects, we adopted a selection criteria based on a galaxy's appearance on the Palomar Observatory Sky Survey "E" and "O" prints.

The cores of rich clusters are dominated by galaxies with Hubble types E and S0 (Bahcall 1977). At the bright end of the luminosity function, the colors of these galaxies are insensitive to luminosity but do vary with redshift, as the spectra shift through the filter bandpasses (Sandage 1973). The brightest cluster members therefore have much the same color. We used this fact to eliminate obvious foreground and background galaxies by estimating a candidate's "E"—"O" color and comparing it to that of the surrounding galaxies. Although imperfect, this technique decreases contamination by non-member galaxies with $|z_{\text{gal}} - z_{\text{cluster}}| \geq 0.03$ (Paper I).

The observations and measurements are summarized in Table 1. The galaxy positions were determined using Kitt Peak two-screw Grant comparitor measurements of the galaxies and SAO reference stars on the Palomar Sky Survey glass copies. The coordinates were derived from the measured positions by

using Don Wells's ASTRO program and have typical standard errors of 2''. Finding charts for the galaxies are presented in Figure 1 (Plates 1–7).

The heliocentric redshifts for the galaxies are listed in column (6). Column (7) denotes the quality of the spectra and the confidence of the measured redshifts. The quality index "A" represents a high signal-to-noise spectrum with all the major spectral and continuum features (Ca H and K, the G-band and the Mg I b-band) easily measurable. A quality index of "B" indicates a well-determined redshift, although one or more of the spectral lines may be poorly defined. Galaxy redshifts listed with a quality index of "C" are based only on one or two possible line identifications and are uncertain. Examples of these confidence ratings have been given in Paper I. In general, these redshifts are accurate to better than $\sim 100 \text{ km s}^{-1}$.

III. THE SURVEYED SUPERCLUSTERS

Table 2 lists all the distance-class 4, 5, and 6 clusters in the field of the investigated superclusters, along with their richness classifications, morphological properties, distance estimates, number of galaxy measurements, and mean redshifts. The estimated redshifts and most Bautz-Morgan classifications (Bautz and Morgan 1970) were taken from Leir and van den Bergh (1977). Column (6) contains the Rood-Sastry morphologies

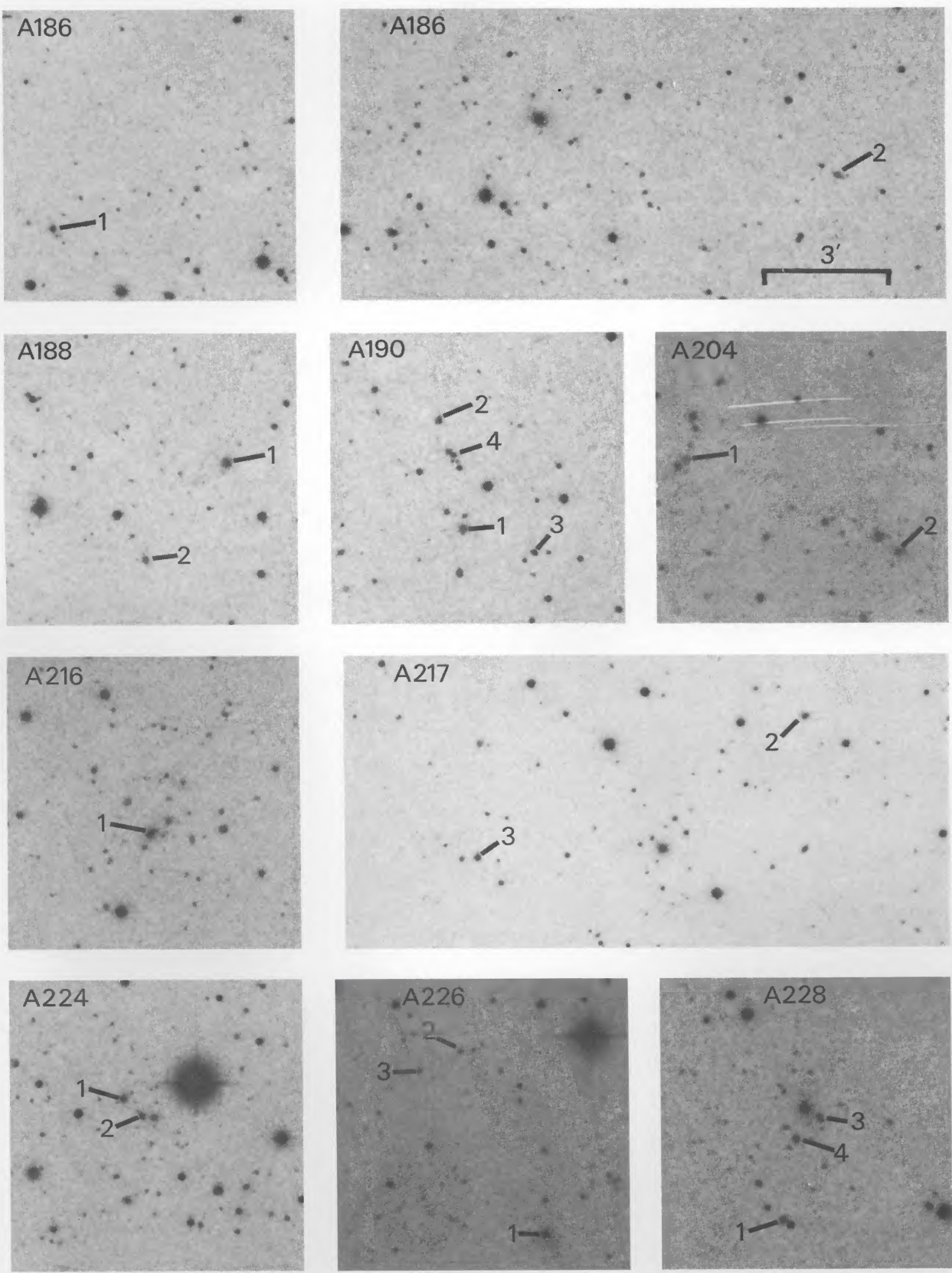


FIG. 1a

FIG. 1.—Finding charts for the measured galaxies in our survey sample of 62 Abell clusters and 11 groups. The charts for Abell clusters 2509, 2521–2540, and 2546–2568 were taken from film copies of the ESO “J” plates. The remaining charts were copied off the Palomar Sky Survey “E” prints. The plate scale is as shown in the finder for Abell 186 and is identical for all clusters.

PLATE 2

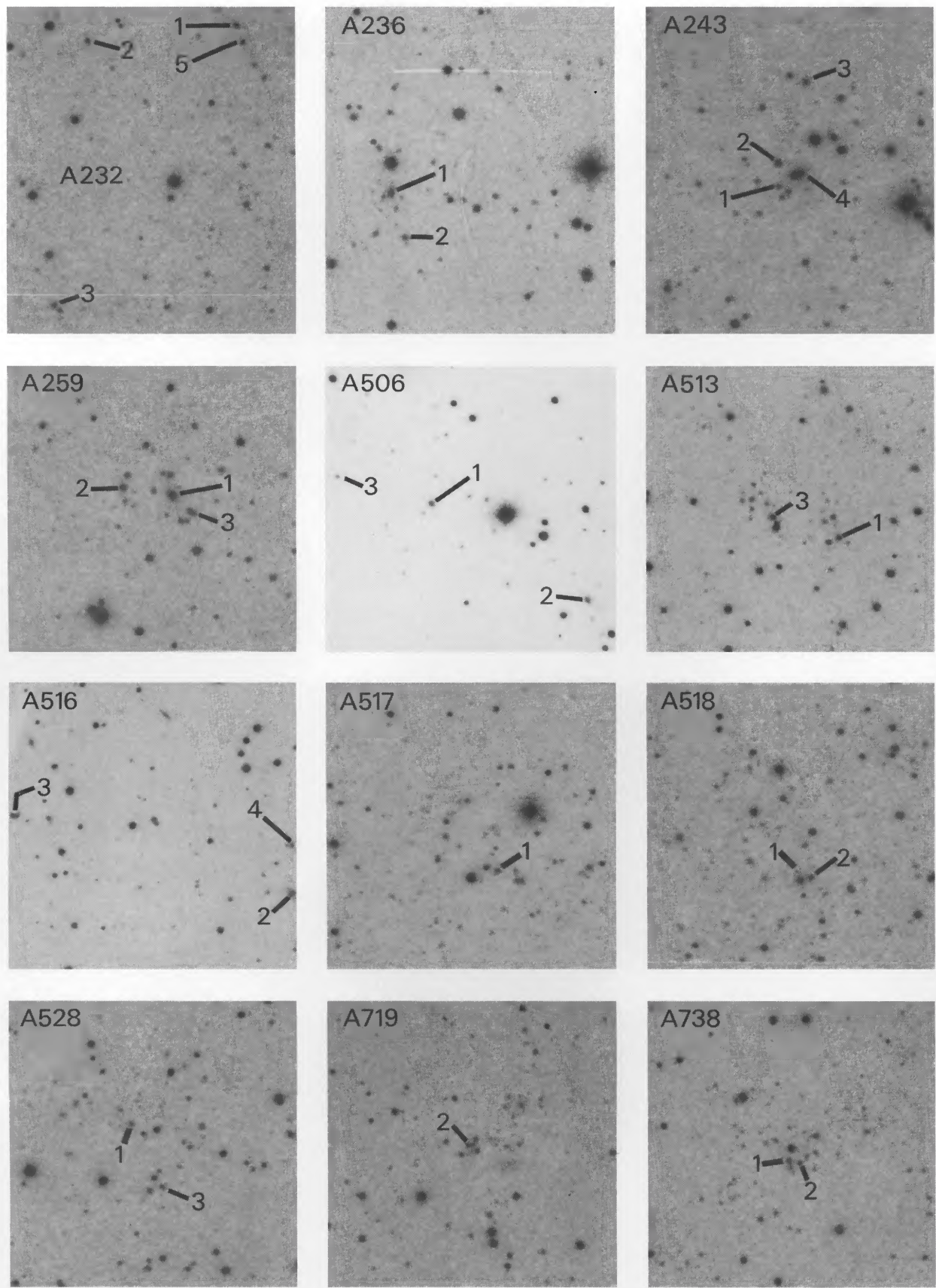


FIG. 1b

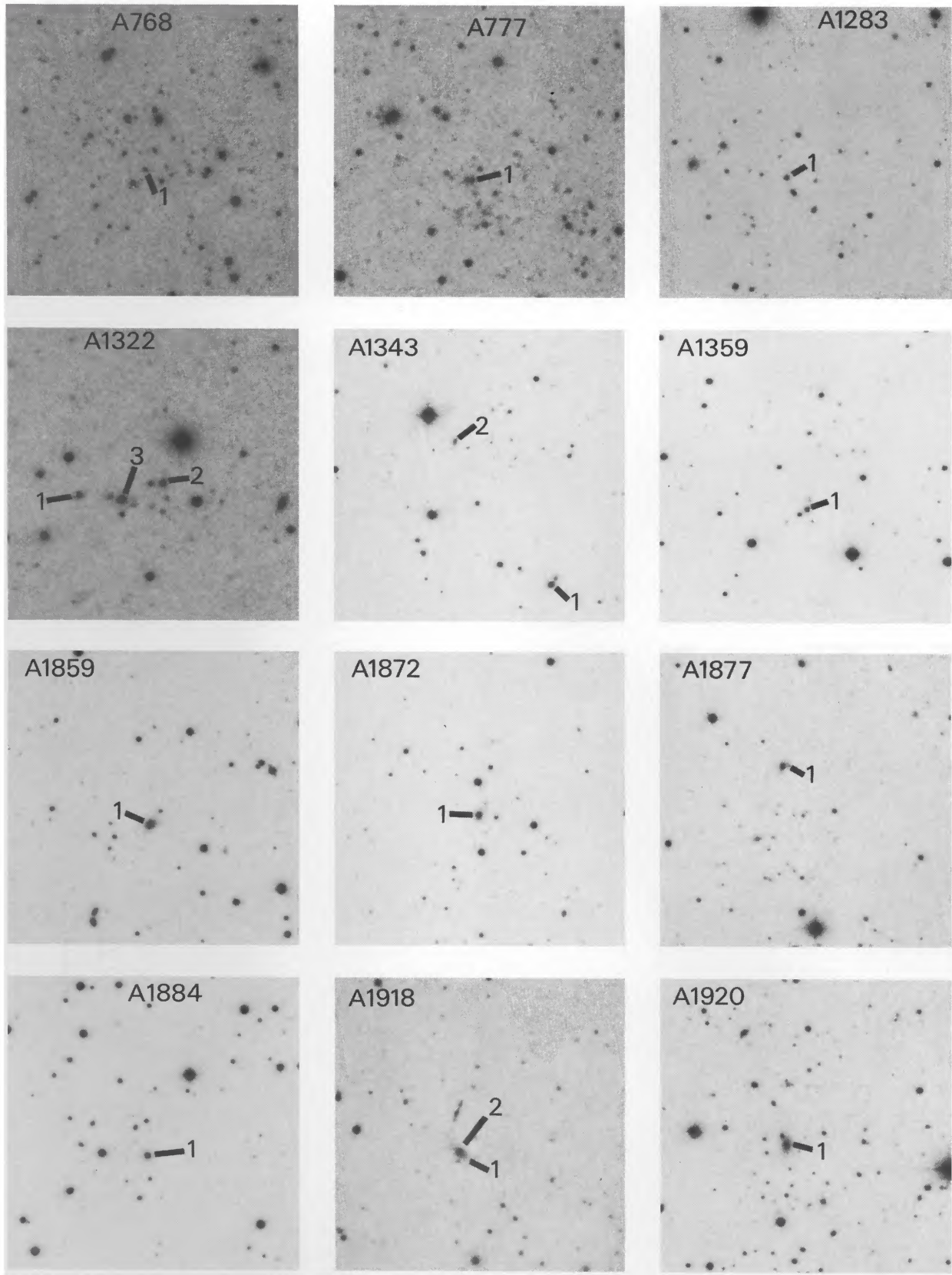


FIG. 1c

CIARDULLO *et al.* (see page 71)

PLATE 4

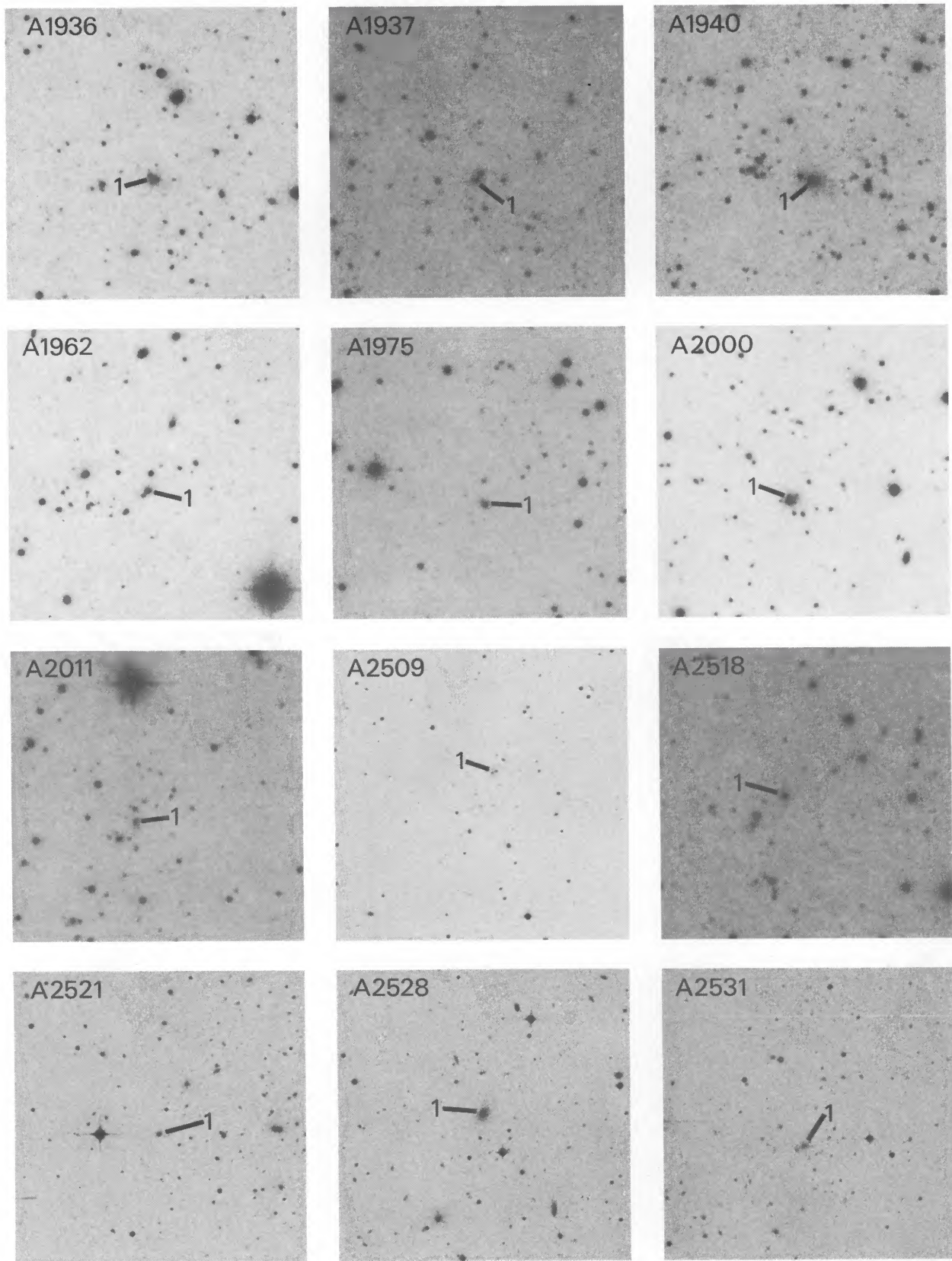


FIG. 1d

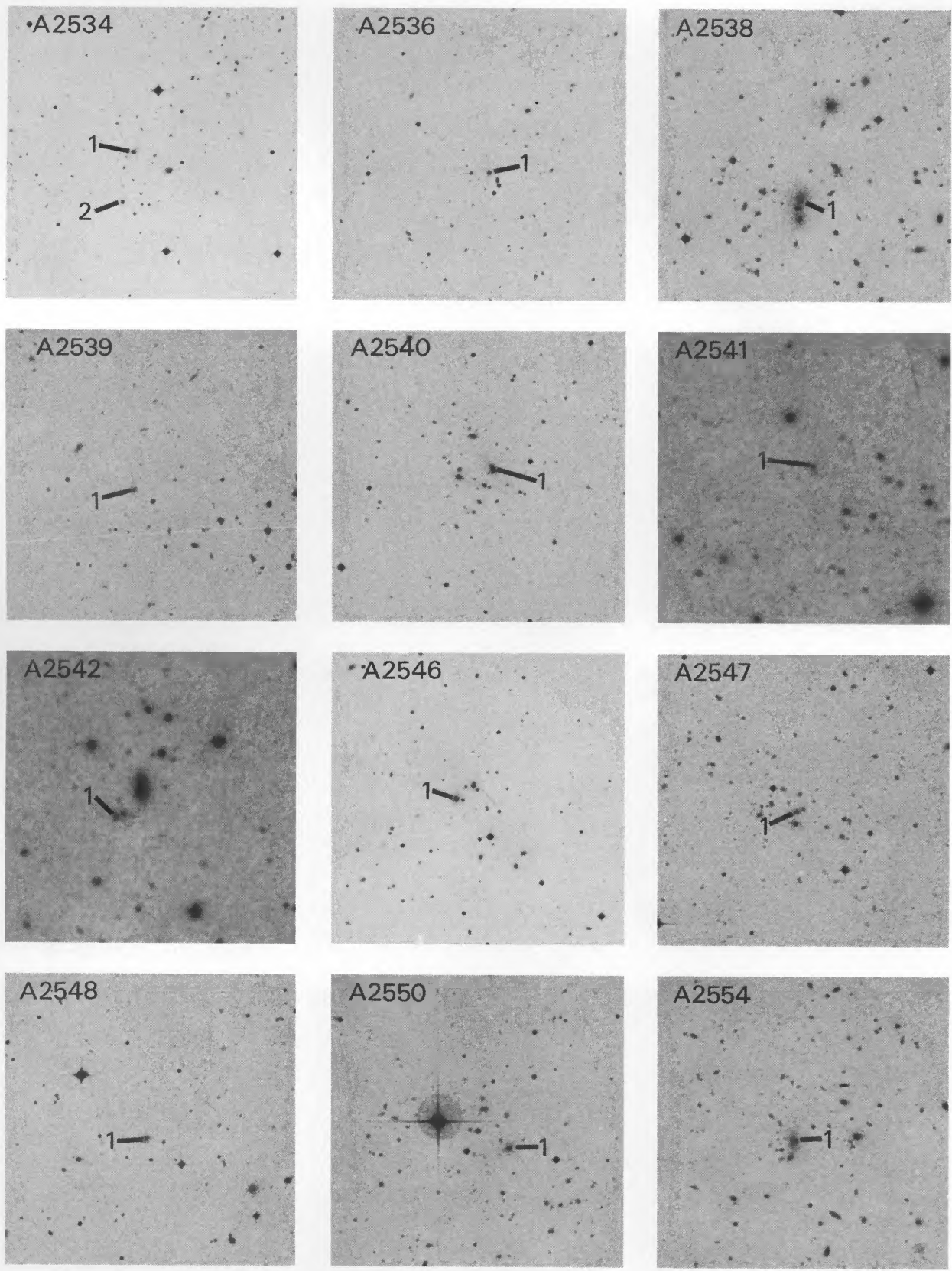


FIG. 1e

CIARDULLO *et al.* (see page 71)

PLATE 6

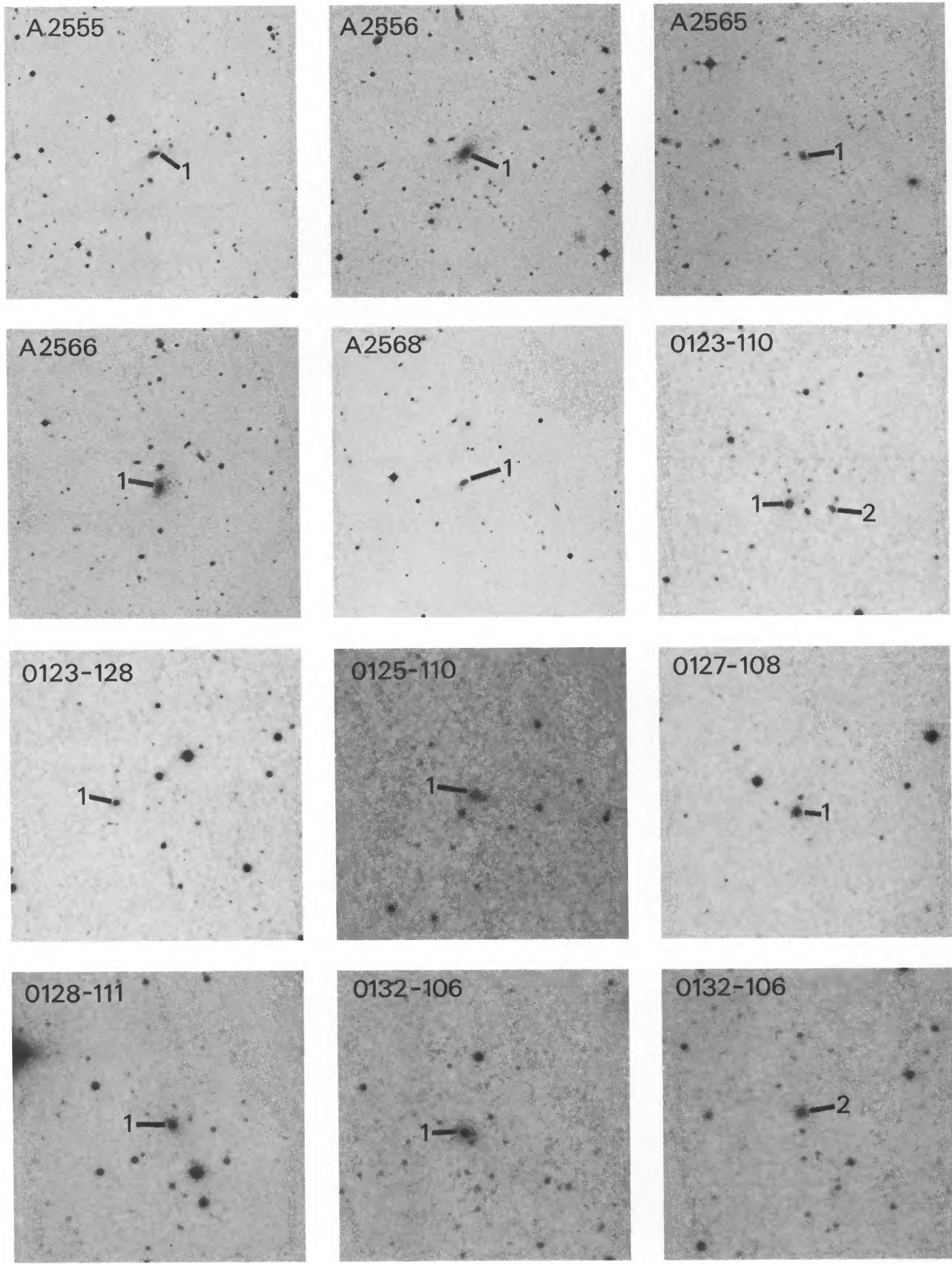


FIG. 1f

CIARDULLO *et al.* (see page 71)

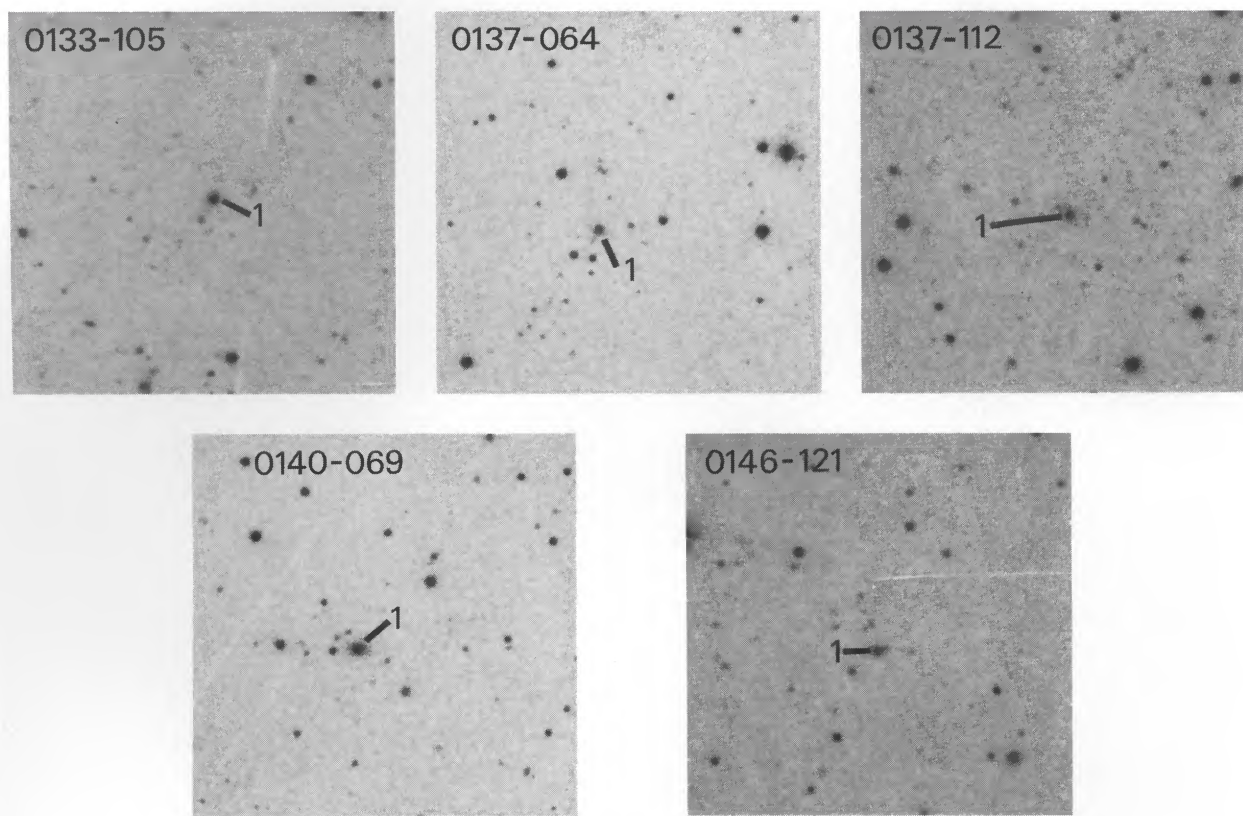


FIG. 1g

CIARDULLO *et al.* (see page 71)

TABLE 2

Cluster (1)	α (1950) (2)	δ (1950) (3)	R (4)	BM (5)	RS (6)	D (7)	z_{est} (8)	N (9)	z (10)
Abell Clusters within 6° of the 0136-10 Field Center									
<i>Association A:</i>									
A226	1 ^h 36 ^m 5	-10°30'	1	II	I	6	0.193	2	0.1282
A228	1 36.7	-10 18	0	II	F	6	...	3	0.1289
A232a	1 37.6	-10 37	1	III:	I	6	0.175	2	0.1329
A259	1 47.8	-12 14	0	II-III	C	5	...	3	0.1273
<i>Association B:</i>									
A216	1 34.2	-6 40	1	II-III	C	5	0.160	1	0.1158
A217	1 34.1	-8 18	1	II:	C:	5	0.138	2	0.1126
A243	1 40.0	-10 29	0	II	B	5	...	4	0.1117
<i>Association C:</i>									
A204b	1 26.1	-7 03	...	III	I	1	0.1870
A232b	1 37.6	-10 37	...	III:	I	2	0.1874
A236	1 38.0	-12 06	1	II-III:	I	5	0.184	2	0.1874
<i>Association D:</i>									
A209	1 29.5	-13 50	3	II-III:	C	6	0.197	1	0.2130
A222	1 35.0	-13 14	3	II-III:	L	6	0.220	1	0.2110
A223	1 35.5	-13 02	3	III	L	6	0.219	2	0.2070
<i>Association E:</i>									
A186b	1 20.2	-10 41	...	III	F	1	0.1538
A204a	1 26.1	-7 03	1	III	F	6	0.165	1	0.1557
<i>Association F:</i>									
A186a	1 20.2	-10 41	1	II	C	5	0.141	2	0.1029
A190	1 21.2	-10 07	0	III	C	5	...	3	0.1015
<i>Other Field Clusters:</i>									
A176	1 17.1	-8 24	1	II-III:	L	6	0.175
A188	1 20.3	-13 02	1	II-III:	I	5	0.171	2	0.1230
A218	1 34.1	-11 00	1	III	F	6	0.264
A224	1 35.8	-7 12	1	III	F	5	0.181	2	0.1617
A230	1 37.0	-11 37	2	III	I	6	0.250
A239	1 38.9	-12 02	2	III	F	6	0.182
A241	1 39.2	-16 30	1	III	I	6	0.257
A242	1 39.5	-14 34	1	I-II	cDp	6	0.257
A251	1 43.9	-7 33	0	III	C	5
A265	1 49.9	-7 16	2	III	F	6	0.236
A274	1 52.2	-6 31	3	III	I	4	0.101	1	0.1290
A282	1 54.5	-10 21	0	III	L	6
Abell Clusters within 6° of the 0446-10 Field Center									
A494	4 ^h 28 ^m 4	-7°51'	2	III	C	6	0.181
A506	4 40.9	-9 48	2	III	I	6	0.148	3	0.1561
A513	4 45.8	-9 48	0	II-III	C	6	0.186	1	0.1491
A516	4 47.7	-8 54	1	II:	I	6	0.165	2	0.1407
A517	4 48.1	-9 19	2	III	I	6	0.179	1	0.2244
A518	4 49.0	-10 48	2	III	F	6	0.166	2	0.1814
A521	4 51.8	-10 20	1	III	L	6	0.200
A522	4 54.6	-6 13	1	III	F	5	0.153
A528	4 56.9	-9 05	0	III	L	6	...	1	0.2896
A536	5 05.4	-9 18	2	III:	F	5	0.160
Abell Clusters within 4° of the 1135+62 Field Center									
A1192	11 ^h 09 ^m 6	59°32'	0	III	I	6
A1221	11 16.9	62 57	1	II:	F	6	0.147
A1239	11 21.1	60 25	0	III	I	6
A1283	11 28.4	61 02	1	III	I	5	0.185	1	0.1434
A1289	11 28.8	61 02	0	III	L	5
A1322	11 34.2	63 30	0	III	L	5	...	3	0.1104
A1324	11 34.4	57 22	1	III	F	5	0.143
A1331	11 36.0	63 52	2	II-III	C	6	0.194
A1343	11 38.6	60 56	0	III:	I	5	...	2	0.1318
A1349	11 39.4	55 38	1	II-III	I	5	0.105
A1351	11 39.8	58 49	2	I-II	cD	6	0.314
A1357	11 40.3	61 34	0	III	F	5
A1359	11 40.8	61 56	0	III	I	5	...	1	0.1783
A1402	11 49.9	60 42	0	III	I	5
A1415	11 53.2	58 09	1	III	L	5	0.155
A1446	11 59.3	58 18	2	II-III	C	5	0.118	1	0.1028
A1496	12 10.9	59 33	1	III	C	4	0.090	1	0.0961

TABLE 2—Continued

Cluster (1)	α (1950) (2)	δ (1950) (3)	R (4)	BM (5)	RS (6)	D (7)	z_{est} (8)	N (9)	z (10)
Abell Clusters within 5° of the 1434 + 58 Field Center									
<i>Association A:</i>									
A1920	14 ^h 25 ^m 7	56°00'	2	II-III:	L	5	0.145	1	0.1310
A1936	14 32.9	55 02	1	III:	C	5	0.164	1	0.1386
A1937	14 33.0	58 29	2	III	F	5	0.193	1	0.1382
A1940	14 33.9	55 22	3	III	F	5	0.130	12	0.1396
<i>Association B:</i>									
A1859	14 03.6	60 20	0	II-III	L	6	...	1	0.0988
A1962	14 41.4	55 25	0	III	I:	5	...	1	0.1060
A1999	14 52.6	54 31	1	II-III	I	4	0.071	1	0.1032
A2000	14 53.1	54 40	1	III	L	5	0.134	1	0.1012
<i>Association C:</i>									
A1877	14 08.9	60 01	1	II	F	6	0.201	1	0.1241
A1884	14 10.4	61 37	0	III	I	6	...	1	0.1220
<i>Other Field Clusters:</i>									
A1776	13 39.2	58 17	0	I	cD	5
A1865	14 04.3	58 54	0	III	I	6
A1872	14 07.6	62 11	0	II	I	5	...	1	0.1508
A1918	14 23.9	63 23	3	I-II	cD	6	0.169	2	0.1386
A1925	14 26.9	57 05	2	II:	C	5	0.166
A1966	14 42.8	59 06	2	III	B	6	0.256
A2013	14 57.6	60 42	2	II:	C	6	0.269
A2015	14 58.2	56 11	1	III:	I	6	0.178
Abell Clusters within 2.5° of the 2306-22 Field Center									
A2509	22 ^h 55 ^m 2	-22°00'	1	III	C	5	0.182	1	0.2306
A2514	22 57.6	-23 28	1	III	C:	6	0.293
A2518	22 58.1	-24 26	1	III	I	5	0.165	1	0.1351
A2521	22 59.6	-22 15	2	I	cDp	5	0.133	2	0.1359
A2526	23 01.4	-24 18	1	III	L	6	0.198
A2528	23 03.0	-21 40	0	III	C	5	...	1	0.0955
A2531	23 04.3	-21 57	1	III	C	5	0.176	1	0.1741
A2534a	23 04.9	-22 56	2	II-III	F	6	0.191	1	0.1997
A2534b	23 04.9	-22 56	...	III	I	1	0.1698
A2536	23 05.1	-22 42	2	III	F	6	0.204	1	0.1971
A2538	23 06.0	-20 09	1	II-III	C	5	0.110	1	0.0817
A2539	23 06.1	-21 45	1	II-III:	I	5	0.115	1	0.1735
A2540	23 06.8	-22 26	1	II:	C	5	0.185	1	0.1297
A2541	23 07.4	-23 14	2	III	I	5	0.153	1	0.1018
A2542	23 07.4	-24 42	1	III	F	5	0.181	1	0.1603
A2546	23 08.1	-22 56	2	II-III	C	5	0.160	1	0.1119
A2547	23 08.2	-21 24	2	III	F	5	0.162	1	0.1492
A2548	23 08.7	-20 42	1	II-III:	I	5	0.134	1	0.1101
A2550	23 08.9	-22 01	2	II-III:	C	5	0.166	1	0.1217
A2554	23 09.8	-21 45	3	II:	cD	5	0.114	1	0.1060
A2555	23 10.1	-22 29	1	II-III	C	5	0.138	1	0.1385
A2556	23 10.4	-21 54	1	II-III:	F	5	0.133	1	0.0879
A2565	23 13.2	-21 23	0	III	F	5	...	1	0.1271
A2566	23 13.3	-20 39	1	III	I	5	0.129	1	0.0821
A2568	23 14.3	-22 28	0	III	I	5	...	1	0.1398

Abell 186.—A186-1 is on the western edge of the cluster proper and is the brightest in a string of faint galaxies extending eastward from the galaxy. The colors and magnitudes of these galaxies strongly suggest that this is a separate system. The listed redshift of the principal cluster is the average of A186-2 and another cluster galaxy observed by Schneider, Gunn, and Hoessel 1983.

Abell 190.—The redshift of A190-2 suggests that it is a member of the principal supercluster. However, it is clearly not associated with the cluster projected in front of it. Without more redshifts, it is impossible to tell whether the galaxy is truly isolated and perhaps just coincidentally at the same redshift of the supercluster, or part of a loose group of galaxies on the eastern edge of the system.

Abell 204.—The “E” – “O” galaxy colors estimated from the Palomar Sky Survey prints indicate that this cluster actually contains two physical associations at different redshifts. The closer of the two systems dominates the center of Abell's defining region and has spurs extending to the north and west. The second, background cluster appears principally in the southeastern section of the field. The two different redshifts obtained reflect this superposition.

Abell 209.—This redshift is taken from Kristian, Sandage, and Westphal 1978.

Abell 222.—This redshift is taken from Westphal, Kristian, and Sandage 1975.

Abell 223.—This redshift is taken from Sandage, Kristian, and Westphal 1976.

Abell 226.—A226-3 is foreground to the main body of the cluster. Its redshift of $z = 0.1144$, however, places it in the foreground supercluster at $z \approx 0.115$. It is possible that this galaxy is associated with Abell 243, which has a redshift of $z \approx 0.112$ and is only ~ 5 Abell radii away.

Abell 232.—The redshifts indicate that this is a superposition of two clusters. The redshifts, however, are too close and most of the galaxies too faint for membership assignments based on estimated colors. As a result, it is impossible to separate the systems or tell which is richer.